1

6

7

8   **A β-mannan utilisation locus in *Bacteroides ovatus* involves a GH36 α-**

9   **galactosidase active on galactomannans**

10   Sumitha K. Reddy[1], Viktoria Bågenholm[1], Nicholas A. Pudlo[2], Hanene Bouraoui[1], Nicole M.

11   Koropatkin[2], Eric C Martens[2], Henrik Stålbrand[1*]

12   [1]Department of Biochemistry and Structural Biology, Lund University,

13   P.O. Box 124, S-221 00, Lund, Sweden

14   [2]Department of Microbiology and Immunology, University of Michigan Medical School, Ann

15   Arbor, Michigan 48109, USA

16   *Corresponding author: E-mail address, henrik.stalbrand@biochemistry.lu.se

17   **ABSTRACT**

18   The *Bacova_02091* gene in the β-mannan utilisation locus of *Bacteroides ovatus* encodes a

19   family GH36 α-galactosidase (BoGal36A), transcriptionally upregulated during growth on

20   galactomannan. Characterisation of recombinant BoGal36A reveals unique properties

21   compared to other GH36 α-galactosidases, which preferentially hydrolyse terminal α-

22   galactose in raffinose family oligosaccharides. BoGal36A prefers hydrolysing internal

23   galactose substitutions from intact and depolymerized galactomannan. BoGal36A efficiently

24 releases (>90%) galactose from guar and locust bean galactomannans, resulting in
25 precipitation of the polysaccharides. As compared to other GH36 structures, the BoGal36A
26 3D model displays a loop deletion, resulting in a wider active site cleft which likely can
27 accommodate a galactose-substituted polymannose backbone.

28 **KEY WORDS**

29 *Bacteroides ovatus*, polysaccharide utilisation locus, GH36 α-galactosidase, galactomannan
30 modification

31

32 **ABBREVIATIONS**

33 PUL: polysaccharide utilisation locus, GH: glycoside hydrolase, CAZy database:
34 carbohydrate active enzyme database, RFOS: raffinose family oligosaccharides, GMOS:
35 galactose substituted manno-oligosaccharides, LBG: locust bean gum, DMSO: dimethyl
36 sulfoxide, IPTG: isopropyl β-D-1-thiogalactopyranoside, GGM: galactoglucomannan,
37 GM_2:6^1-α-D-galactosyl-mannobiose, GM_3: 6^1-α-D-galactosyl-mannotriose, G_2M_5: 6^3,6^4-α-
38 D-galactosyl-mannopentaose, *p*NP-α-gal: p-nitrophenyl-α-galactopyranoside, HPAEC-PAD:
39 high performance anion exchange chromatography with pulsed amperometric detection, SEC:
40 size exclusion chromatography, DLS: dynamic light scattering.

41

42 **INTRODUCTION**

43 α-Galactosidases have been classified in glycoside hydrolase (GH) families GH4, GH27,
44 GH36, GH57, GH97 and GH110 based on their sequence similarity, see the Carbohydrate
45 Active Enzymes database (www.cazy.org) [1]. GH27 and GH36 α-galactosidases belong to
46 clan D and share a common $(\alpha/\beta)_8$ fold [2]. These families contain cloned and some
47 structurally characterised α-galactosidases from various prokaryotic and eukaryotic organisms
48 isolated from soil [3-5], thermal springs [6, 7] and the mammalian gut [8-10]. GH27 α-
49 galactosidases are active on both terminal and/or internal galactosidic linkages from
50 polysaccharides like galactomannan [11] and galactosylated oligosaccharides [4], while GH36
51 α-galactosidases are mainly active on terminal α-galactosidic linkages in raffinose family
52 oligosaccharides (RFOS) such as raffinose and melibiose [8, 10, 12]. Previous studies suggest

53 that unique structural/sequence motifs and the oligomeric state of the enzymes impart the

54 substrate preferences (terminal vs internal galactose linkages) in GH27 [4] and GH36 [12] α-

55 galactosidases. Tetrameric α-galactosidases from both the families have a narrow active site

56 cleft and preferably hydrolyse only terminal α-galactosidic linkages present in RFOS [4, 12].

57 Recent phylogenetic analysis of GH36 enzymes clusters these sequences into 4 distinct

58 subgroups [8]. The GH36 subgroup I is by far the largest group of the family and contains

59 mainly tetrameric α-galactosidases active on terminal α-galactosidic linkages. The majority of

60 biochemically and structurally characterised subgroup I α-galactosidases [8] are from gut

61 bacteria such as *Bifidobacterium* and *Lactobacillus* species and are involved in RFOS

62 utilisation [8, 12-15]

63 By bioinformatics analysis we discovered a putative GH36 α-galactosidase gene

64 (*Bacova_02091*) encoded by a recently discovered polysaccharide utilization locus (PUL)

65 [16] implicated in β-mannan utilization by the gut bacterium *Bacteroides ovatus* ATCC 8483.

66 In this study, we cloned the gene and characterized the corresponding α-galactosidase

67 (BoGal36A). In contrast to GH27 α-galactosidases, GH36 α-galactosidases have not

68 previously been shown to have significant activity towards galactosylated polymeric β-

69 mannans (i.e. being able to hydrolyse galactosyl substitutions attached to internal mannose

70 units) [3, 17]. Our analysis revealed that BoGal36A belongs to GH36 subgroup I, but has

71 distinct structural and catalytic features associated with β-mannan utilization rather than

72 RFOS utilization, which is the case for other subgroup I α-galactosidases as described above.

73 In addition, we relate this knowledge to other *Bacteroides* species, including *B. fragilis* which

74 recently was proposed to catabolise β-mannan via a new pathway [18].

MATERIALS AND METHODS

Growth and transcriptional analysis of *Bacteroides* species on β-mannans

77 The *Bacteroides* strains tested were grown in tryptone-yeast extract-glucose (TYG) medium

78 [19] or on brain-heart infusion (BHI; Beckton Dickinson) agar containing 10% horse blood

79 (Colorado Serum Co.). Growth measurements on individual substrates were performed in

80 minimal medium (MM) containing a single carbohydrate at 5 mg/ml (w/v) final concentration

81 in 96-well format using an automated absorbance reader as previously described [16].

82 Transcriptional activation of the *B. ovatus* ATCC 8483 galactomannan PUL on LBG

83　galactomannan and konjac glucomannan was derived from normalized Affymetrix GeneChip

84　data as described in [16].

BoGal36A sequence analysis

86　The gene sequence of *Bacova_02091* (GenBank: EDO12201.1, UniProt ID: A7LW87) was

87　mined from genomic sequence data of *B. ovatus* ATCC 8483 for primer design and cloning. A

88　BLASTP search with the protein sequence BoGal36A was performed on the UniProtKB

89　(http://www.uniprot.org/blast/) and PDB databases. Presence of signal peptide was analysed

90　on the signal P server (http://www.cbs.dtu.dk/services/SignalP/) [20]. A basic phylogenetic

91　tree was constructed using all the characterized protein sequences from GH36 displayed in the

92　CAZy database along with BoGal36A using maximum likelihood analysis on MEGA 6.0

93　[21]. Multiple sequence alignments of BoGal36A with structurally characterised α-

94　galactosidases from GH36 subgroup I was performed with the T-coffee tool

95　(http://www.ebi.ac.uk/Tools/msa/tcoffee/). The alignment was processed in ESPript3.0 [22]

96　and was presented with secondary structure from the crystal structure of *Geobacillus*

97　*stearothermophillus* α-galactosidase (AgaB: PDBID-4FNQ) [10] as reference.

Cloning of *Bacova_02091* from *Bacteriodes ovatus* ATCC 8483

99　The *Bacova_02091* gene encoding BoGal36A was amplified by the polymerase chain reaction

100　(PCR) from genomic DNA of *B. ovatus* ATCC 8483, prepared as described previously [19].

101　Primers were designed to include Nco1 and Xho1 sites for cloning. PCR reaction of 50 μl was

102　set up containing $MgCl_2$ (2 mM), DNA (5 ng), dNTPs (250 μM), 0.5 μM primers (forward

103　primer: 5´ATACCATGGCCCAAAATATACATTTGTCAACC and reverse primer:

104　5´CGTCTCGAGCT TAACCTCTTCCAGATAAAGTA), dimethyl sulfoxide (DMSO) (2%),

105　and *Pfu* DNA polymerase (2.5 U). The conditions used for PCR were: first cycle at 95 °C for

106　5 min followed by 35 cycles at 95 °C for 30 s, 55 °C for 30 s and 72 °C for 2 min, and a final

107　cycle at 72 °C for 5 min. The PCR product was double digested by Nco1 and Xho1 enzymes

108　(Thermo scientific) and cloned into these sites of the pET28b+ expression vector to generate a

109　clone pB2091 for expression of BoGal36A protein with C-terminal His_6 tag. The positive

110　clones containing pB2091 plasmid were confirmed by sequencing and further transformed

111　into a calcium competent BL21 (DE3) *E. coli* strain for BoGal36A expression.

BoGal36A expression and characterisation

113   *E.coli* BL21 cells containing the pB2091 plasmid, encoding for the BoGal36A protein, was

114   cultured in Luria Bertani media at 37 °C. The recombinant protein expression was induced by

115   addition of 1 mM isopropyl β-D-1-thiogalactopyranoside (IPTG) at mid exponential phase

116   ($O.D_{600nm} \approx 0.7$). The cells were harvested after incubation at 37 °C for 4 hours. BoGal36A

117   was initially released from the induced BL21 cells by suspending the cells in binding buffer

118   (20 mM Tris-HCl, pH 8.0, 300 mM NaCl, 10 mM imidazole, 1 mM phenyl methyl sulphonyl

119   flouride) and lysing it with glass beads (2 µm diameter, Biospec) by vortexing for 10 times

120   with intervals of 30 s on ice. The supernatant after centrifugation of the lysate at 15,000 rpm

121   for 20 min was loaded on 2 ml His tag resin pre-equilibrated with the binding buffer. After

122   overnight binding at 4 °C the column was washed with wash buffer (20 mM Tris-HCl, pH 8.0,

123   300 mM NaCl, 50 mM imidazole) and BoGal36A was eluted in elution buffer (20 mM Tris-

124   HCl, pH 8.0, 300 mM NaCl, 200 mM imidazole). Pure fractions were pooled and buffer was

125   exchanged to 50 mM citrate buffer pH 6.0. Protein concentration was measured on a nano

126   drop ND 1000 spectrophotometer at 280 nm. Absorbances were correlated to the protein

127   concentrations based on the theoretical extinction coefficient: $144675 M^{-1} cm^{-1}$. The theoretical

128   molecular weight and the molar extinction coefficient were obtained from the ProtParam tool

129   (http://web.expasy.org/) using the protein sequence of BoGal36A. The eluted protein fractions

130   were also analysed on SDS PAGE (Techtum, 4-12%).

131   Size-exclusion chromatography (SEC) was performed to identify the oligomeric state of

132   BoGal36A. 500µl of 2mg/ml BoGal36A, was loaded on 16/60 Superdex 200 (GE healthcare)

133   pre-equilibrated with 50mM citrate buffer pH 6.0 at a flow rate of 0.5 mL/min connected to

134   ÄKTA system (GE healthcare). 500µl of γ-thyroglobulin 669 kDa, apoferritin 443kDa and β-

135   amylase 200kDa (MWGF1000, Sigma-Aldrich), was used as molecular weight standards.

136   Two injections of BoGal36A eluted with identical volumes. The apparent molecular weight of

137   oligomeric BoGal36A was calculated based on the calibration curve obtained by plotting

138   partition coefficient (K_{av}) vs log molecular weight of standard proteins.

139   **Substrates**

140   The following were purchased from Sigma: the artificial substrates p-nitrophenyl-α-

141   galactopyranoside (*p*NP-α-gal), p-nitrophenyl-α-glucopyranoside (*p*NP-α-gluc), p-

142   nitrophenyl-β-galactopyranoside (*p*NP-β-gal), p-nitrophenyl-β-glucopyranoside (*p*NP-β-gluc)

143   and p-nitrophenyl-β-arabinopyranoside (*p*NP-β-ara). RFOS: raffinose, melibiose and

144   stachyose. Galactomannan polysaccharides (β-1, 4 linked mannan backbone with α-1, 6

145 linked galactose substitutions): locust bean gum and guar gum (galactose:mannose ratio ~1:4
146 and ~1:2, respectively) [11]. Galactosylated manno-oligosaccharides (GMOS) are products
147 from hydrolytic galactomannan depolymerisation and were purchased from Megazyme
148 International (Bray, Ireland): 6^1-α-D-Galactosyl-mannobiose (GM$_2$), 6^1-α-D-Galactosyl-
149 mannotriose (GM$_3$) and 6^3, 6^4-α-D-Galactosyl-mannopentaose (G$_2$M$_5$). Galactoglucomannan
150 (GGM) was prepared as described previously [23].

Activity assay and α-galactosidase specificity

152 The standard α-galactosidase assay was performed using 1 mM pNP-α-gal and release of p-
153 nitrophenol was measured at 405 nm after incubation with BoGal36A at 37 ℃, in 50 mM pH
154 6.0 sodium citrate buffer. The reaction was stopped after 10 min with 1 M Na$_2$CO$_3$. Assays
155 using pNP-α-gluc, pNP-β-gal, pNP-β-gluc or pNP-β-ara were performed under similar
156 conditions. The pH optimum was determined by the standard activity assay using buffers
157 between pH 2.0-9.0. The buffers used were 50 mM glycine-HCl buffer for pH 2.0-3.0, 50 mM
158 sodium-citrate buffer for pH 4.0-5.0, 50 mM citrate-phosphate buffer for pH 6.0-7.0 and 50
159 mM Tris-HCl buffer for pH 8.0-9.0. Temperature optimum was also determined by standard
160 activity assay at five different temperatures 4 ℃, 30 ℃, 37 ℃, 50 ℃ and 70 ℃. Incubations
161 were also done for 24 hours at various pH and temperatures to determine the pH and
162 temperature stabilities. Michaelis-Menten kinetics was done with pNP-α-gal as substrate by
163 continuous assay. 0.1 mM to 5 mM concentration of pNP-α-gal was incubated with 0.1 mg/ml
164 of BoGal36A. The rate of the reaction was calculated by monitoring the release of
165 paranitrophenol at 405 nm for 5 min. K_M and k_{cat} values were obtained by fitting the rate of
166 the reaction and substrate concentration in a Michaelis–Menten equation. All the reactions
167 were done in duplicates.

Substrate specificity using oligo- and polysaccharides

169 RFOS (raffinose, melibiose, stachyose) and GMOS (GM$_2$, GM$_3$, G$_2$M$_5$) were incubated with
170 BoGal36A and analysed for galactose release. 500 nM of enzyme was incubated with 5 mM
171 of each oligosaccharide in a total volume of 500 µl for maximum of 12 hours.
172 Polysaccharides (0.5% Locust bean gum, guar gum or acetylated GGM) were also incubated
173 with 1 µM of enzyme in a total volume of 500 µl. Aliquots of 150 µl were taken at 1 hour, 3
174 hours and 12 hours and the samples were analysed for galactose release by high performance
175 anion exchange chromatography with pulsed amperometric detection (HPAEC-PAD)

176 (Dionex, Sunnyvale, CA) on a PA10 column with 1% NaOH isocratic elution [24]. Specific

177 activity and extent of galactose released from polysaccharides were calculated based on the

178 galactose release after 1 hour and 12 hours respectively. All the reactions were done in

179 duplicates.

180 **k_{cat}/K_m analysis on GMOS and RFOS**

181 50 µM of GMOS (GM$_2$, GM$_3$ and G$_2$M$_5$) and RFOS (melibiose, stachyose, raffinose) were

182 incubated with BoGal36A (34.2 nM for GMOS and 85.2 nM for RFOS) in 50 mM sodium

183 citrate buffer pH 6.0 at 37ºC. The total reaction volume was 750 µl and aliquots of 125 µl

184 were taken at 0, 2, 5, 10, 20 and 30 min for each of the substrates and the reaction was

185 stopped by addition of 10 µl 5 % NaOH. All the reactions were done in duplicates. The

186 decrease in substrate concentration for each of the GMOS and RFOS was analysed by

187 HPAEC-PAD on a PA100 column as described previously [25]. k_{cat}/K_M was calculated

188 according to the Matsui equation [26] by plotting Ln (S_o/S_t) as a function of time (t) similar to

189 previous studies [24]. S_o is the initial substrate concentration at time zero, and S_t is the

190 substrate concentration at time (t).

191 **DLS analysis and guar gum aggregation**

192 The ability of BoGal36A to modify the size of guar gum aggregates was followed by dynamic

193 light scattering (DLS) experiments. 500 µl reaction volume was set up with 0.25% guar gum

194 in 50 mM citrate buffer pH 6.0 and 0.1 mg/ml of BoGal36A enzyme. The reaction was carried

195 out in a micro-volume quartz cuvette at 37ºC in a zeta sizer-Nano ZS90 (Malvern

196 instruments). The change in particle size in the reaction mixture was followed every 10 min

197 for 16 hours. The particle size of the polysaccharide was measured as Z_{ave} mean on zeta sizer

198 (Nano ZS90), based on the absorption at 488 nm. Z_{ave} mean is the mean size diameter

199 calculated by considering all the other factors like viscosity, Boltzmann constant and diffusion

200 [27, 28]. It more accurately represents the particle size during the course of reaction. Aliquots

201 of 20 µl were taken at four different time points: 0 hours, 4 hours, 12 hours and 16 hours to

202 analyse the galactose release at different time intervals on HPAEC-PAD PA10 column. The

203 % galactose released was calculated based on the galactose: mannose ratio of 0.7:1 in guar

204 gum.

205 **Homology model**

206 A homology model of BoGal36A was built in Swiss PDB model work space
207 (http://swissmodel.expasy.org/) using the crystal structure (chain A) of a α-galactosidase from
208 *Geobacillus stearothermophillus* AgaA (PDBID - 4FNP) [10], with 34% sequence identity as
209 template. The quality of the 3D model was assessed based on Q mean score and gave a Z
210 value of - 0.576. Ramachandran plot analysis showed 0.5% of amino acid residues in
211 disallowed regions, 97% of residues in the allowed region and 1.5% in generously allowed
212 regions. All the figures were drawn in PyMOL (Molecular Graphics 122 System, Version
213 1.5.0.4 Schrödinger, and LLC).

RESULTS

215 The genetic loci proposed to be involved in β-mannan utilization in *B. ovatus* ATCC8483
216 (Type 1, Fig 1A) and *B. fragilis* NCTC 9343, respectively, are shown in Fig 1 A. It can be
217 concluded that the loci lack overall homology, one of the differences being absence of a
218 possible α-galactosidase gene for *B. fragilis*. On the other hand, we found that *B.*
219 *xylanisolvens D 22* has a genetic locus (HMPREF0106_00419 to HMPREF0106_00429) with
220 overall homology to the type 1 locus of *B. ovatus*. Growth studies on galactomannan substrate
221 shows that at least some of the tested *B. ovatus* and *B. xylanisolvens* strains efficiently utilise
222 galactomannan as a substrate, while none of the tested *B. fragilis* species were able to grow on
223 galactomannan (Fig 1B), including the type strain *B. fragilis* NCTC 9343. Comparative
224 genomic analysis of the sequenced *B. ovatus* and *B. xylanisolvens* strains with high growth on
225 galactomannan (Fig 1B) showed presence of a genetic locus homologous to type 1 β-mannan
226 PUL of *B. ovatus* ATCC 8483 (Fig 1A, and SFig 1). Transcriptional activation analysis for
227 growth of *B. ovatus* ATCC 8483 on galactomannan showed upregulation of the type 1 β-
228 mannan utilisation locus (gene cluster *Bacova_02087-97),* (Fig 1C).This gene cluster contains
229 the GH36 α-galactosidase gene, locus tag *Bacova_02091,* along with two putative GH26 β-
230 mannanase genes (locus tags *Bacova_02092* and *Bacova_02093*) and a putative GH130
231 gluco-mannophosphorylase (locus tag *Bacova_02090*). Some of the *B. ovatus* strains with
232 positive growth on galactomannan lack the type 1 β-mannan PUL, but have a partially
233 homologous PUL (Type 2), which however lacks a α-galactosidase (Fig 1A, B and SFig 1). α-
234 Galactosidase activity is needed for hydrolysis of galactosyl substitutions present in
235 galactomannans, albeit this is a function known for GH27 but not for GH36 α-galactosidases,
236 as explained above. Presence of a GH36 α-galactosidase gene in a β-mannan PUL motivated
237 us to clone and study the properties of the recombinant enzyme BoGal36A.

Sequence analysis of BoGal36A

238

239 BoGal36A has an N-terminal signal peptide but no lipid anchor attachment. The protein is

240 thus predicted to be secretory and soluble. Its potential presence in periplasm or extracellular

241 environment is, however, difficult to predict. A BlastP search using the sequence of

242 BoGal36A as a query resulted in many putative α-galactosidases from *Bacteroides* species.

243 The highest identity (36%) for a characterised α-galactosidase was that from a symbiotic

244 bacterium *Flavobacteria sp.* TN17 isolated from the gut of the wood feeding insect *Batocera*

245 *horsefeldi* [29]. The phylogenetic analysis clusters BoGal36A to subgroup I [12] of GH36,

246 which contains the majority of structurally and biochemically characterised α-galactosidases

247 from raffinose utilisation loci of other gut bacteria (SFig 2). The sequence alignment with

248 structurally characterised GH36 α-galactosidases from subgroup I indicate conserved amino

249 acids involved in galactose recognition and a GXXLXXXG motif unique for α-galactosidases

250 from subgroup I (Fig 2) proposed to be involved in protein tetramerisation [12].

251 **Cloning and basic characterisation**

252 The gene sequence encoding BoGal36A without the predicted secretion signal was amplified

253 from genomic DNA of *B ovatus* ATCC 8483 and cloned into the pET28b+ vector with a C-

254 terminal His_6 tag. The overexpressed protein was purified by His-Tag purification. A single

255 band corresponding to ≈ 81 kDa , observed on SDS PAGE (SFig 3) was similar to the

256 theoretical molecular weight of BoGal36A (80.7 kDa). In SEC analysis, BoGal36A elutes as a

257 single peak at 61.3 ml (SFig 4) which corresponds to 290 kDa, slightly below the theoretical

258 molecular weight of a tetramer (324kDa).

259 Recombinant BoGal36A is active on *p*NP-α-gal, but not on the other tested *p*NP-glycosides.

260 Thus, basic characterisation was done with *p*NP-α-gal as substrate. BoGal36A has pH

261 optimum of 6.0 and optimum temperature of 50 ºC (Fig 3B) over an assay time of 10 min but

262 is not stable if the incubation is prolonged. However, the enzyme retains greater than 85%

263 activity at pH 6.0 (Fig 3C) when incubated at 37 ºC for 24 hours. Thus, the optimum

264 conditions of pH 6.0 and 37 ºC were used in further incubations for analysis of kinetic

265 parameters and natural substrate specificity. BoGal36A has K_m of 0.132 ± 0.02 mM and k_{cat}

266 of 4774 ± 202 min^{-1} using *p*NP-α-gal as substrate.

267 **Substrate specificity on galactose containing substrates**

268   The specific activities for the galactomannans guar gum and LBG and for GGM are $64.2 \pm$

269    $3.7 \ min^{-1}$, $70.2 \pm 6.96 \ min^{-1}$ and $9.6 \pm 0.3 \ min^{-1}$ respectively. BoGal36A had a higher specific

270   activity of $1260 \pm 32 \ min^{-1}$ on G_2M_5. Both the galactose residues were released from G_2M_5

271   (Fig 4A) and a single galactose group was released from GM_2 and GM_3. Galactose was also

272   released from RFOS (melibiose, raffinose, stachyose), but less efficiently than from GM_2,

273   GM_3 and G_2M_5 as shown by substrate depletion curves (Fig 4B). About 90% of galactose

274   was   released   from   LBG   and   guar   gum   galactomannan   after   incubating   0.5%   of

275   polysaccharides (Fig 4C and D). Precipitation of guar galactomannan was observed due to

276   aggregation of polysaccharide backbone after galactose removal. Only 10 % galactose was

277   removed from GGM.

278   **k_{cat}/K_m analysis: Terminal vs internal galactose specificity**

279   BoGal36A hydrolyses internally linked α-1, 6 galactose residues from the GMOS: GM_2,

280   GM_3, and G_2M_5 with 13 times higher catalytic efficiency (k_{cat}/K_m) compared to terminal α-

281   galactose residues from the RFOS raffinose, stachyose and melibiose (Fig 4B and Table 1). It

282   has similar catalytic efficiency for GM_2, GM_3 and G_2M_5, indicating that the length of the

283   mannan backbone or the frequency of galactose substitutions does not affect the catalytic

284   efficiency of the enzyme. In contrast, for RFOS the catalytic efficiency decreases for raffinose

285   and stachyose compared to melibiose (Table 1). Based on k_{cat}/K_m analysis it can be ventured

286   that BoGal36A can accommodate mannosyl substituted galactose (GMOS) in the active site

287   better than galactosylated oligosaccharides from the RFOS family.

288   **DLS experiments for guar gum aggregation.**

289   Addition   of   BoGal36A   actively   removes   the   galactosyl   residues   from   guar   gum

290   galactomannan, thus promoting aggregation of mannan backbone. Initially, the guar gum

291   galactomannan has a particle size diameter between 10 nm and 100 nm (Fig 5B). Removal of

292   galactose substitutions resulted in aggregation and the increase in particle size to 1 μm is

293   proportional to the extent of galactose removal (Fig 5). The graph plotted (Fig 5A) shows the

294   change in particle size of guar gum galactomannan displayed as Z_{ave} mean vs time during the

295   course of galactose removal by BoGal36A. The real time change in particle size is shown in

296   Fig 5B and 5C for 0 hours and 16 hours, respectively. At 4 hours, where the galactose

297   removal was less than 40%, the change in particle size was not significant. The galactose

298 removal reached 65% at 8 hours and there was a steady increase in Z_{ave}. The particle size

299 increased to ≈1 μm after 16 hours when the extent of galactose release reached 90%.

Homology model

301 The observed differences for BoGal36A (not optimal RFOS activity, rather active on

302 galactomannan and GMOS) and other gut bacterial GH36 α-galactosidases (involved in

303 RFOS hydrolysis) led us to try to find structural differences. The BoGal36A 3D model was

304 based on the template structure of AgaA from *G. stearothermophillus*, which is tetrameric in

305 solution [10]. The tetrameric BoGal36A model was generated assuming that the orientation of

306 the individual monomers in the modeled BoGal36A is similar to that of AgaA. Comparison

307 using an active site overlay of modeled BoGal36A showing raffinose bound in the active site

308 of AgaA (PDB: FN0) indicates a conserved -1 subsite involved in galactose recognition as

309 compared to the template (Fig 6).

310 The main differences are seen in the +1 and +2 subsites of AgaA. The P related-loop (AgaA

311 amino acids 55-66) of the AgaA structure is absent in BoGal36A (Fig 6). This loop provides

312 stacking and hydrogen bonding substrate interactions (to Glu and Frc moieties of raffinose)

313 via residues in the +1 and +2 subsites (AgaA amino acids Phe 56, Arg65, Asp53) [10].

314 Furthermore, we made a structural overlay of all structurally characterised GH36 subgroup I

315 α-galactosidases (the same as used Fig. 2) which are preferentially active on terminal α-

316 galactosidic linkages. The P-loop is spatially conserved in all these α-galactosidases (i.e.

317 except BoGal36A) and restricts the space in the positive subsites of the active site cleft. The

318 absence of the loop in BoGal36A is likely to provide additional space for a polymannose

319 backbone and/or allow accommodation of galactose substitutions.

DISCUSSION

321 Gene clusters implicated in β-mannan utilisation have been suggested for some *Bacteriodes*

322 species and a few other bacteria which occur in the human gut [16, 18, 30, 31]. However, only

323 limited data is available on the functional proteins involved in the utilisation of

324 galactomannan as carbon source in such bacteria [32-35]. *B. ovatus* has previously been

325 shown to utilise galactomannan as a carbon source [16, 33]. α-Galactosidases have been

326 characterised from *B. ovatus* grown on galactomannan [32, 33]. However, no genomic data or

327 sequence data is available relating the activity to protein sequences, GH family or genetic

locus. In the current study we show that the *B. ovatus* β-mannan PUL [16] includes a gene for a GH36 α-galactosidase (BoGal36A) transcriptionally upregulated, along with the PUL, during growth on galactomannan (Fig 1C). The genetic co-regulation and the biochemical characterisation of BoGal36A suggest a new role for a GH36 α-galactosidase, i.e. in galactomannan degradation, a function rather observed for GH27 enzymes from bacteria and fungi [3, 36].

BoGal36A belongs to GH36 α-galactosidases subgroup I, hitherto suggested to contain enzymes that mainly have evolved to hydrolyse RFOS substrates with a narrow active site formed by enzyme tetramers [10, 12]. Interestingly, while being tetrameric, BoGal36A is more efficient in removing internal galactosidic linkages from GMOS of DP 2-5, compared to RFOS (Table 1), and also releases 90% galactose from guar gum and LBG galactomannans, which is not shown for any other characterised GH36 α-galactosidase. Previously characterised, but unidentified, α-galactosidases from *B. ovatus* cannot hydrolyse galactose residues from intact galactomannans [32, 37]. An overlay of the modelled tetrameric BoGal36A active site with that of the active site of the RFOS-hydrolysing AgaA α-galactosidase reveals likely architectural differences between BoGal36A and other subgroup I GH36 enzymes. The absence of a loop in the N terminal region (residues 50-66, AgaA numbering) of BoGal36A, containing aromatic residues involved in stacking interactions in the positive subsites of AgaA, can likely provide the additional space to accommodate galactose substitution carried by a polymannose backbone (Fig 6).

As it appears, BoGal36A has evolved to hydrolyse internal galactosyl decorations from GMOS and/or galactomannans, an activity previously known for GH27 α-galactosidases that act synergistically with β-mannanases for effective galactomannan utilisation [11, 38]. The β-mannan PUL upregulated in presence of galactomannan (Fig 1C) also encodes two putative GH26 β-mannanases along with BoGal36A (Fig 1A). Known β-mannanases hydrolysing galactomannans by endo-action are often restricted by galactosyl substitution present on the β-mannan chain [2, 39, 40]. The transcriptional regulator (*Bacova_02097*) of the *B. ovatus* β-mannan PUL, is also sensitive to galactosyl substitutions, and cannot bind di-galactosyl mannopentaose (G_2M_5) but can bind undecorated β-mannan oligosaccharides [16]. In line with these observations, it's likely that the function of BoGal36A is removal of internal galactose residues from galactomannans and/or GMOS produced by the putative β-mannanases, enabling the effective utilisation of galactomannan as the carbon source.

360   Additionally, BoGal36A can also be effectively utilised as a biotechnological tool for
361   modifying the properties of galactomannans (Fig 5).

362   Exo-glycosidases such as BoGal36A, described in this study may play an essential role in the
363   *Bacteroidetes* ability to utilise several heteroglycans, acting together with endohydrolases that
364   depolymerise glycan backbones. As an example, exoglycosidases belonging to GH31 (α-
365   xylosidases) and GH2 (β-galactosidases) were shown to play an important role in xyloglucan
366   utilisation of *B. ovatus* [19]. Recently, α-mannan utilisation in *B. thetaiotamicron* was
367   described and also involves exo-acting GHs such as a α-1, 6 mannosidase acting together with
368   endo-acting GHs to effectively utilise the highly branched yeast α-mannan as carbon source
369   [41].

370   **CONCLUSION**

371   This study gives insight into the GHs involved in the β-mannan utilisation of *Bacteroides*
372   species, with focus on the potential role of a GH36 α-galactosidase, evolved to hydrolyse the
373   internal galactose residues of galactomannan substrates. Based on the genomic context and
374   the substrate preferences of BoGal36A it can be hypothesised that BoGal36A act in
375   cooperation with the predicted GH26 β-mannanase(s) of the same PUL for effective
376   galactomannan utilisation. The competitive environment in the gut may be a contributing
377   factor to the evolution of the structural-functional difference of BoGal36A compared to the
378   characterised homologs in subgroup I of GH36. Furthermore, the study also exemplifies that
379   the human gut microbiome can be mined for novel enzymes e.g. for certain applications; in
380   this case for the degalactosylation of galactomannans.

381   **ACKNOWLEDGEMENTS**

385   **CONTRIBUTIONS**

386   HS, NK and EM defined the overall research topic. HS, NK, EM and SKR planned the study.
387   SKR, NAP, VB and HB conducted experiments. All authors interpreted the data. SKR, HS,
388   VB, NK and EM wrote the MS.

REFERENCES

1. Cantarel, B. L., Coutinho, P. M., Rancurel, C., Bernard, T., Lombard, V. & Henrissat, B. (2009) The Carbohydrate-Active EnZymes database (CAZy): an expert resource for Glycogenomics, *Nucleic Acids Res.* **37**, D233-8.

2. Gilbert, H. J., Stalbrand, H. & Brumer, H. (2008) How the walls come crumbling down: recent structural biochemistry of plant polysaccharide degradation, *Current Opinion in Plant Biology.* **11**, 338-348.

3. Ademark, P., de Vries, R. P., Hagglund, P., Stalbrand, H. & Visser, J. (2001) Cloning and characterization of Aspergillus niger genes encoding an alpha-galactosidase and a beta-mannosidase involved in galactomannan degradation, *Eur J Biochem.* **268**, 2982-90.

4. Fernandez-Leiro, R., Pereira-Rodriguez, A., Cerdan, M. E., Becerra, M. & Sanz-Aparicio, J. (2010) Structural analysis of Saccharomyces cerevisiae alpha-galactosidase and its complexes with natural substrates reveals new insights into substrate specificity of GH27 glycosidases, *J Biol Chem.* **285**, 28020-33.

5. Shankar, S. K., Dhananjay, S. K. & Mulimani, V. H. (2009) Purification and characterization of thermostable alpha-galactosidase from Aspergillus terreus (GR), *Appl Biochem Biotechnol.* **152**, 275-85.

6. King, M. R., Yernool, D. A., Eveleigh, D. E. & Chassy, B. M. (1998) Thermostable alpha-galactosidase from Thermotoga neapolitana: cloning, sequencing and expression, *FEMS Microbiol Lett.* **163**, 37-42.

7. Comfort, D. A., Bobrov, K. S., Ivanen, D. R., Shabalin, K. A., Harris, J. M., Kulminskaya, A. A., Brumer, H. & Kelly, R. M. (2007) Biochemical analysis of Thermotoga maritima GH36 alpha-galactosidase (TmGalA) confirms the mechanistic commonality of clan GH-D glycoside hydrolases, *Biochemistry.* **46**, 3319-30.

8. Abou Hachem, M., Fredslund, F., Andersen, J. M., Larsen, R. J., Majumder, A., Ejby, M., Van Zanten, G., Lahtinen, S. J., Barrangou, R., Klaenhammer, T., Jacobsen, S., Coutinho, P. M., Lo Leggio, L. & Svensson, B. (2012) Raffinose family oligosaccharide utilisation by probiotic bacteria: insight into substrate recognition, molecular architecture and diversity of GH36 alpha-galactosidases, *Biocatalysis and Biotransformation.* **30**, 316-325.

9. Aguilera, M., Rakotoarivonina, H., Brutus, A., Giardina, T., Simon, G. & Fons, M. (2012) Aga1, the first alpha-Galactosidase from the human bacteria Ruminococcus gnavus E1, efficiently transcribed in gut conditions, *Res Microbiol.* **163**, 14-21.

10. Merceron, R., Foucault, M., Haser, R., Mattes, R., Watzlawick, H. & Gouet, P. (2012) The molecular mechanism of thermostable alpha-galactosidases AgaA and AgaB explained

by x-ray crystallography and mutational studies, *The Journal of biological chemistry.* **287**, 39642-52.

11. Moreira, L. R. & Filho, E. X. (2008) An overview of mannan structure and mannan-degrading enzyme systems, *Appl Microbiol Biotechnol.* **79**, 165-78.

12. Fredslund, F., Hachem, M. A., Larsen, R. J., Sorensen, P. G., Coutinho, P. M., Lo Leggio, L. & Svensson, B. (2011) Crystal structure of alpha-galactosidase from Lactobacillus acidophilus NCFM: insight into tetramer formation and substrate binding, *Journal of molecular biology.* **412**, 466-80.

13. Bruel, L., Sulzenbacher, G., Cervera Tison, M., Pujol, A., Nicoletti, C., Perrier, J., Galinier, A., Ropartz, D., Fons, M., Pompeo, F. & Giardina, T. (2011) alpha-Galactosidase/sucrose kinase (AgaSK), a novel bifunctional enzyme from the human microbiome coupling galactosidase and kinase activities, *The Journal of biological chemistry.* **286**, 40814-23.

14. Carrera-Silva, E. A., Silvestroni, A., LeBlanc, J. G., Piard, J. C., Savoy de Giori, G. & Sesma, F. (2006) A thermostable alpha-galactosidase from Lactobacillus fermentum CRL722: genetic characterization and main properties, *Curr Microbiol.* **53**, 374-8.

15. Hirayama, Y., Sakanaka, M., Fukuma, H., Murayama, H., Kano, Y., Fukiya, S. & Yokota, A. (2012) Development of a double-crossover markerless gene deletion system in Bifidobacterium longum: functional analysis of the alpha-galactosidase gene for raffinose assimilation, *Applied and environmental microbiology.* **78**, 4984-94.

16. Martens, E. C., Lowe, E. C., Chiang, H., Pudlo, N. A., Wu, M., McNulty, N. P., Abbott, D. W., Henrissat, B., Gilbert, H. J., Bolam, D. N. & Gordon, J. I. (2011) Recognition and degradation of plant cell wall polysaccharides by two human gut symbionts, *PLoS Biol.* **9**, e1001221.

17. Centeno, M. S., Guerreiro, C. I., Dias, F. M., Morland, C., Tailford, L. E., Goyal, A., Prates, J. A., Ferreira, L. M., Caldeira, R. M., Mongodin, E. F., Nelson, K. E., Gilbert, H. J. & Fontes, C. M. (2006) Galactomannan hydrolysis and mannose metabolism in Cellvibrio mixtus, *FEMS Microbiol Lett.* **261**, 123-32.

18. Senoura, T., Ito, S., Taguchi, H., Higa, M., Hamada, S., Matsui, H., Ozawa, T., Jin, S., Watanabe, J., Wasaki, J. & Ito, S. (2011) New microbial mannan catabolic pathway that involves a novel mannosylglucose phosphorylase, *Biochem Biophys Res Commun.* **408**, 701-6.

19. Larsbrink, J., Rogers, T. E., Hemsworth, G. R., McKee, L. S., Tauzin, A. S., Spadiut, O., Klinter, S., Pudlo, N. A., Urs, K., Koropatkin, N. M., Creagh, A. L., Haynes, C. A., Kelly, A.

G., Cederholm, S. N., Davies, G. J., Martens, E. C. & Brumer, H. (2014) A discrete genetic locus confers xyloglucan metabolism in select human gut Bacteroidetes, *Nature.* **506**, 498-502.

20.	Petersen, T. N., Brunak, S., von Heijne, G. & Nielsen, H. (2011) SignalP 4.0: discriminating signal peptides from transmembrane regions, *Nat Methods.* **8**, 785-6.

21.	Tamura, K., Stecher, G., Peterson, D., Filipski, A. & Kumar, S. (2013) MEGA6: Molecular Evolutionary Genetics Analysis version 6.0, *Molecular biology and evolution.* **30**, 2725-9.

22.	Robert, X. & Gouet, P. (2014) Deciphering key features in protein structures with the new ENDscript server, *Nucleic Acids Research.* **42**, W320-W324.

23.	Lundqvist, J., Jacobs, A., Palm, M., Zacchi, G., Dahlman, O. & Stalbrand, H. (2003) Characterization of galactoglucomannan extracted from spruce (Picea abies) by heat-fractionation at different conditions, *Carbohyd Polym.* **51**, 203-211.

24.	Reddy, S. K., Rosengren, A., Klaubauf, S., Kulkarni, T., Karlsson, E. N., de Vries, R. P. & Stalbrand, H. (2013) Phylogenetic analysis and substrate specificity of GH2 beta-mannosidases from Aspergillus species, *Febs Lett.* **587**, 3444-9.

25.	Ademark, P., Lundqvist, J., Hagglund, P., Tenkanen, M., Torto, N., Tjerneld, F. & Stalbrand, H. (1999) Hydrolytic properties of a beta-mannosidase purified from Aspergillus niger, *Journal of biotechnology.* **75**, 281-9.

26.	Matsui, I., Ishikawa, K., Matsui, E., Miyairi, S., Fukui, S. & Honda, K. (1991) Subsite Structure of Saccharomycopsis Alpha-Amylase Secreted from Saccharomyces-Cerevisiae, *J Biochem-Tokyo.* **109**, 566-569.

27.	Parikka, K., Leppanen, A. S., Pitkanen, L., Reunanen, M., Willfor, S. & Tenkanen, M. (2010) Oxidation of Polysaccharides by Galactose Oxidase, *J Agr Food Chem.* **58**, 262-271.

28.	Chimphango, A. F. A., van Zyl, W. H. & Gorgens, J. F. (2012) In situ enzymatic aided formation of xylan hydrogels and encapsulation of horse radish peroxidase for slow release, *Carbohyd Polym.* **88**, 1109-1117.

29.	Zhou, J., Shi, P., Huang, H., Cao, Y., Meng, K., Yang, P., Zhang, R., Chen, X. & Yao, B. (2010) A new alpha-galactosidase from symbiotic Flavobacterium sp. TN17 reveals four residues essential for alpha-galactosidase activity of gastrointestinal bacteria, *Appl Microbiol Biotechnol.* **88**, 1297-309.

30.	Kawahara, R., Saburi, W., Odaka, R., Taguchi, H., Ito, S., Mori, H. & Matsui, H. (2012) Metabolic mechanism of mannan in a ruminal bacterium, Ruminococcus albus, involving two mannoside phosphorylases and cellobiose 2-epimerase: discovery of a new carbohydrate

491 phosphorylase, beta-1,4-mannooligosaccharide phosphorylase, *The Journal of biological*
492 *chemistry.* **287**, 42389-99.

493 31. McNulty, N. P., Wu, M., Erickson, A. R., Pan, C., Erickson, B. K., Martens, E. C., Pudlo,
494 N. A., Muegge, B. D., Henrissat, B., Hettich, R. L. & Gordon, J. I. (2013) Effects of diet on
495 resource utilization by a model human gut microbiota containing Bacteroides cellulosilyticus
496 WH2, a symbiont with an extensive glycobiome, *PLoS biology.* **11**, e1001637.

497 32. Gherardini, F., Babcock, M. & Salyers, A. A. (1985) Purification and characterization of
498 two alpha-galactosidases associated with catabolism of guar gum and other alpha-galactosides
499 by Bacteroides ovatus, *J Bacteriol.* **161**, 500-6.

500 33. Valentine, P. J. & Salyers, A. A. (1992) Analysis of proteins associated with growth of
501 Bacteroides ovatus on the branched galactomannan guar gum, *Applied and environmental*
502 *microbiology.* **58**, 1534-40.

503 34. Kulcinskaja, E., Rosengren, A., Ibrahim, R., Kolenova, K. & Stalbrand, H. (2013)
504 Expression and characterization of a Bifidobacterium adolescentis beta-mannanase carrying
505 mannan-binding and cell association motifs, *Applied and environmental microbiology.* **79**,
506 133-40.

507 35. Morrill, J., Kulcinskaja, E., Sulewska, A. M., Lahtinen, S., Stalbrand, H., Svensson, B. &
508 Abou Hachem, M. (2015) The GH5 1,4-beta-mannanase from Bifidobacterium animalis
509 subsp. lactis Bl-04 possesses a low-affinity mannan-binding module and highlights the
510 diversity of mannanolytic enzymes, *BMC biochemistry.* **16**, 26.

511 36. Kim, W. D., Kobayashi, O., Kaneko, S., Sakakibara, Y., Park, G. G., Kusakabe, I.,
512 Tanaka, H. & Kobayashi, H. (2002) alpha-Galactosidase from cultured rice (Oryza sativa L.
513 var. Nipponbare) cells, *Phytochemistry.* **61**, 621-30.

514 37. Valentine, P. J., Gherardini, F. C. & Salyers, A. A. (1991) A Bacteroides ovatus
515 chromosomal locus which contains an alpha-galactosidase gene may be important for
516 colonization of the gastrointestinal tract, *Applied and environmental microbiology.* **57**, 1615-
517 23.

518 38. Malgas, S., van Dyk, J. S. & Pletschke, B. I. (2015) A review of the enzymatic hydrolysis
519 of mannans and synergistic interactions between beta-mannanase, beta-mannosidase and
520 alpha-galactosidase, *World J Microbiol Biotechnol.* **31**, 1167-75.

521 39. Gherardini, F. C. & Salyers, A. A. (1987) Purification and characterization of a cell-
522 associated, soluble mannanase from Bacteroides ovatus, *Journal of bacteriology.* **169**, 2038-
523 43.

524   40.   Gherardini, F. C. & Salyers, A. A. (1987) Characterization of an outer membrane

525   mannanase from Bacteroides ovatus, *Journal of bacteriology.* **169**, 2031-7.

526   41. Cuskin, F., Lowe, E. C., Temple, M. J., Zhu, Y., Cameron, E. A., Pudlo, N. A., Porter, N.

527   T., Urs, K., Thompson, A. J., Cartmell, A., Rogowski, A., Hamilton, B. S., Chen, R., Tolbert,

528   T. J., Piens, K., Bracke, D., Vervecken, W., Hakki, Z., Speciale, G., Munoz-Munoz, J. L.,

529   Day, A., Pena, M. J., McLean, R., Suits, M. D., Boraston, A. B., Atherly, T., Ziemer, C. J.,

530   Williams, S. J., Davies, G. J., Abbott, D. W., Martens, E. C. & Gilbert, H. J. (2015) Human

531   gut Bacteroidetes can utilize yeast mannan through a selfish mechanism, *Nature.* **517**, 165-9.

532   .

533

534   **Figure 1**: ***Bacteroides* genes involved in galactomannan degradation and growth of**

535   **selected species on β-mannans.** (A) Gene clusters from *B. ovatus* (Type 1) and *B. fragilis*

536   (bottom) that have previously been implicated in β-mannan degradation [16, 18]. Type 2

537   putative β-mannan PUL was discovered in the current study. Surrounding genes that were not

538   shown to be transcriptionally active in response to β-mannan (for *B. ovatus*) / or were not

539   tested for functions in β-mannan degradation are showed as partially transparent. Note that

540   flanking *BF0771-74* there is a GH26-containing polysaccharide utilisation locus. (B) Growth

541   of strains from 3 different *Bacteroides* species on LBG galactomannan. Growth ability of the

542   strains with Type 1 PUL is highlighted in red (*B. ovatus* ATCC *8483* is indicated by an

543   arrow), strains with Type 2 PUL are marked in pink. Sequenced *B. ovatus* and *B.*

544   *xylanisolvens* strains with no growth on galactomannan do not contain either of the PULs.(C)

545   Transcriptional activation of the *B. ovatus* ATCC *8483 Bacova_02087-97,* Type 1 β-mannan

546   PUL on konjac glucomannan and LBG galactomannan. More information related to strains

547   numbers and the homologous/partially homologous PULs is presented in supplementary

548   material (STable 1, SFig 1)

549   **Figure 2: Multiple alignment of structurally characterised GH36 α-galactosidases from**

550   **Subgroup I.** The subgroup classification is based on Fredslund et al [12] and secondary

551   structure elements from GH36 α-galactosidase from *G. stearothermophillus*: PDB ID 4FNQ.

552   Completely conserved residues are marked black and partially conserved residues are marked

553   as grey. Catalytic amino acids: nucleophile D479 and acid/base D549 are marked. Unique

554   features: **(A)** missing loop in BoGal36A **(B)** CXXGXXR motif involved in galactose

555   recognition in subgroup1 and **(C)** GXXLXXXG motif involved in tetramer formation in
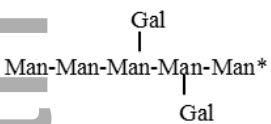556   subgroup I.

557   **Figure 3: Effect of pH and temperature on activity of BoGal36A: (A)** pH optimum:
558   hydrolysis of *p*NP- α-gal for 10 min at pH 2-9. **(B)** Temperature optimum: hydrolysis of *p*NP-
559   α-gal at pH 6 for 10 min**. (C)** pH stability: activity dependence from pH 3-9 for 24 hours at 37
560   ℃**(D)** Temperature stability: activity dependence at pH 6 for 24 hours at 30 ℃, 37 ℃, 50 ℃.

561   **Figure 4: Galactose release analysis: (A)** G_2M_5 hydrolysed to M_5, analysed on PA100
562   column. (---) indicates G_2M_5 at 0 hours. Mannose standards M2-M5 and galactose peak is
563   also indicated. **(B)** Degradation curves for galactose substituted oligosaccharides. (¨)
564   indicates RFOS (—) indicates GMOS. Markers indicate (●) GM_2, (♦) GM_3, (■) G_2M_5, (Δ)
565   melibiose (□) Raffinose and (○) stachyose**.** Galactose release analysed on PA10 column for
566   BoGal36A hydrolysed guar gum **(C)** and locust bean gum **(D)**. Grey indicates 1 mM galactose
567   standard. Black line indicates galactose release from polysaccharides and bold black line
568   indicates sample at 0 hours.

569   **Figure 5: DLS analysis of guar gum galactomannan: (A)** mean particle size distribution
570   (Z_{ave}) of guar gum with galactose removal by BoGal36A over time for 16 hours**.** The real
571   time change in particle size is shown for 0 hours **(B)** and 16 hours **(C)**. In initial time points at
572   4 hours, where the galactose removal is less than 40%, the change in particle size is not
573   significant. The particle size increases to≈1 μm after 16 hours when the extent of galactose
574   release reached 90%.

575   **Figure 6: Close up view of BoGal36A overlay on AgaA with raffinose bound in the**
576   **active site pocket [10]:** Amino acids from the template structure AgaA (red), with raffinose
577   (yellow) in the active site, and the BoGal36A model (blue). Phe 56, Asp 53 and Arg 65
578   (labeled red, AgaA numbering) are part of the loop that is lacking in BoGal36A. The positive
579   and negative subsites are marked as -1, +1 and +2 respectively. Amino acids involved in
580   galactose recognition at the -1 subsite are conserved and are underlined (BoGal36A
581   numbering).

Table 1: Kinetic properties of BoGal36A on different galactose substrates

| Substrate	Structure	k_{cat}/K_m (M^{-1} Min^{-1})
pNp-α-gal		$3.6 \times 10^7 \pm 8.9 \times 10^5$
RFOS		
Raffinose	αGal-(1,6)-αGlc*	$2.6 \times 10^5 \pm 2.2 \times 10^4$
Melibiose	αGal(1,6)-αGlc-(1,2)-βFru	$5.16 \times 10^4 \pm 1.7 \times 10^3$
Stachyose	αGal(1,6)-αGal(1,6)-αGlc-(1,2)-βFru	$3.16 \times 10^4 \pm 2.2 \times 10^3$
GMOS		
GM$_2$	Gal | Man-Man*	$3.5 \times 10^6 \pm 1.0 \times 10^5$
GM$_3$	Gal | Man-Man-Man*	$3.24 \times 10^6 \pm 1.7 \times 10^5$
G$_2$M$_5$	Gal | Man-Man-Man-Man-Man* | Gal	$3.15 \times 10^6 \pm 2.3 \times 10^5$

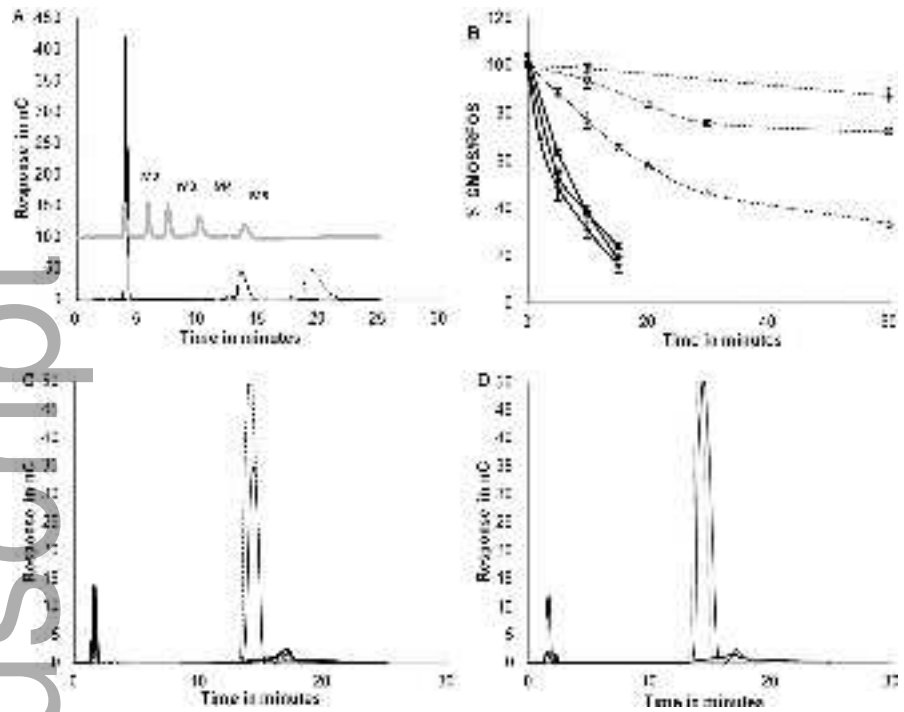* Represents reducing end of the oligosaccharide
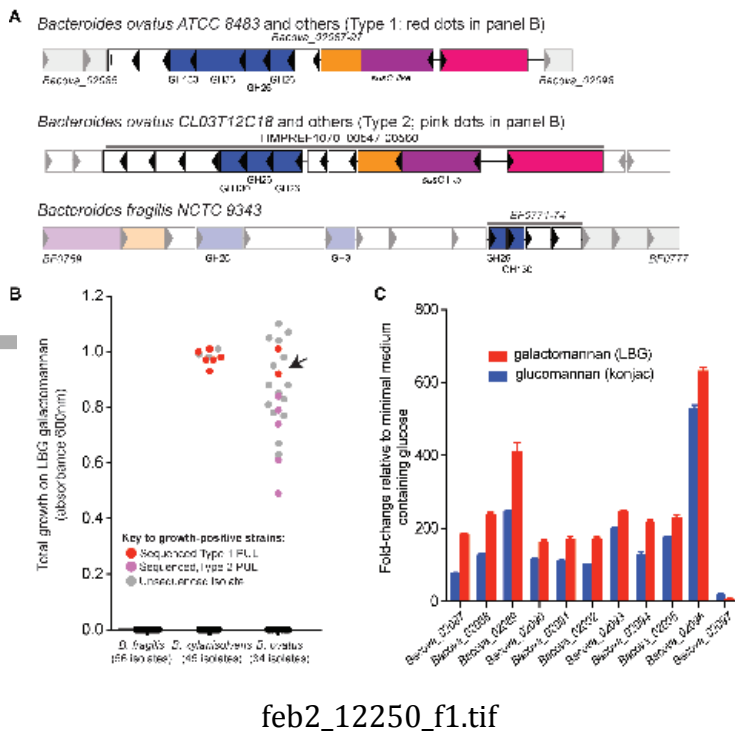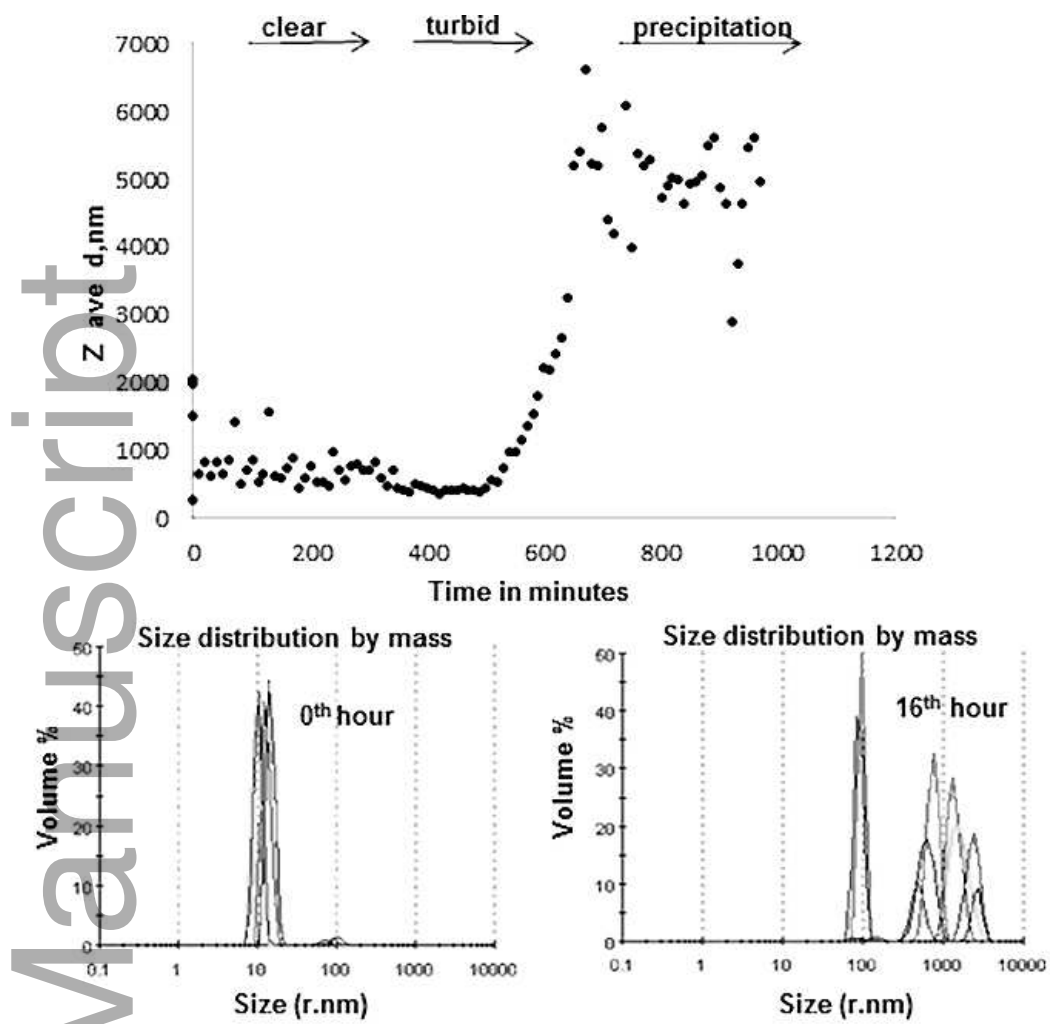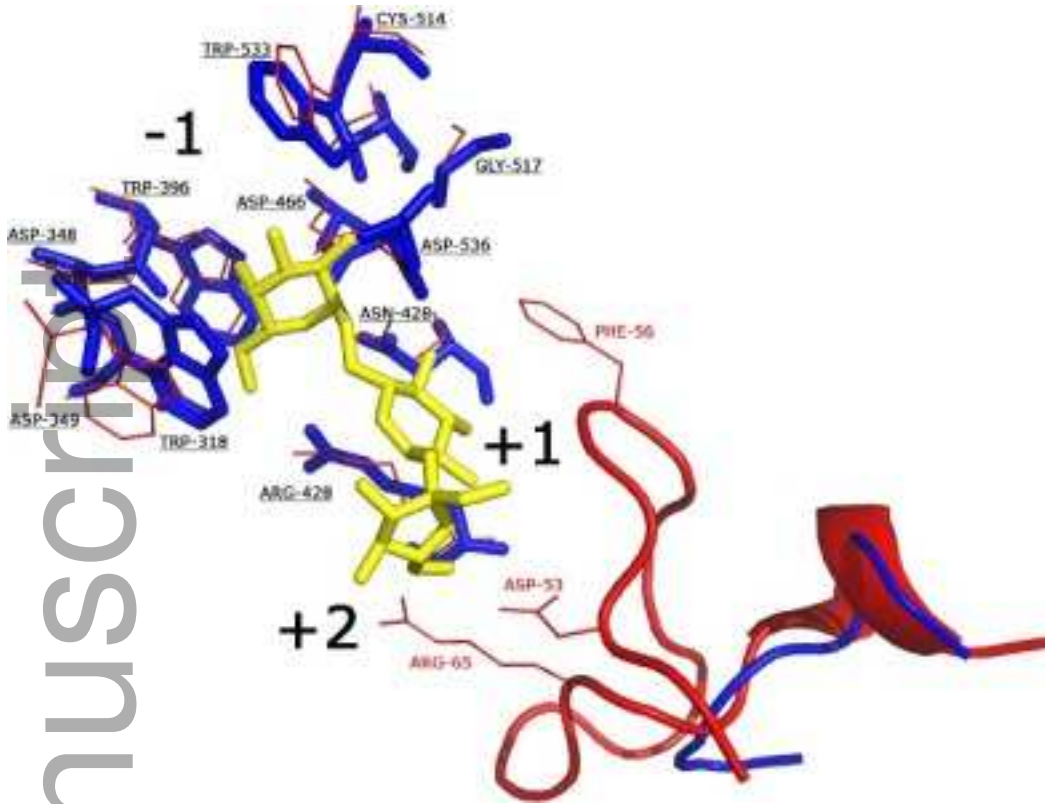
feb2_12250_f1.tif
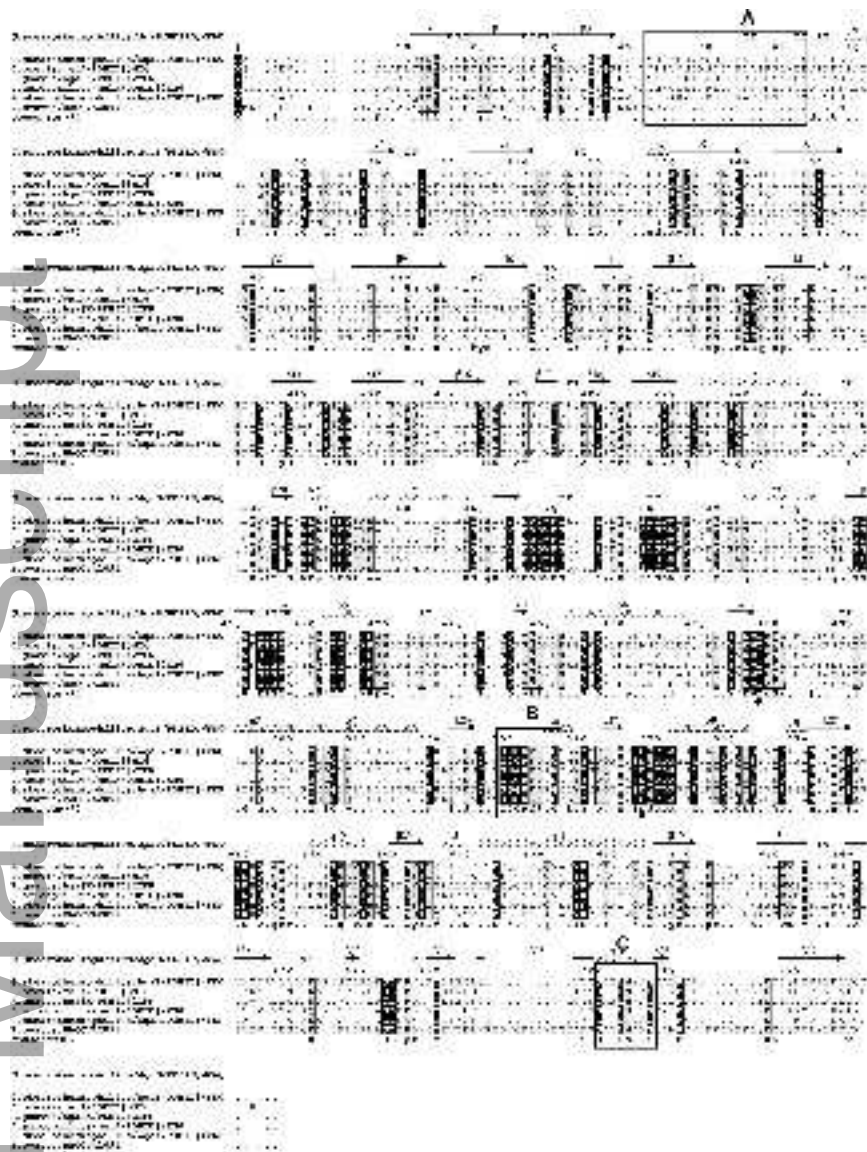
feb2_12250_f2.tif
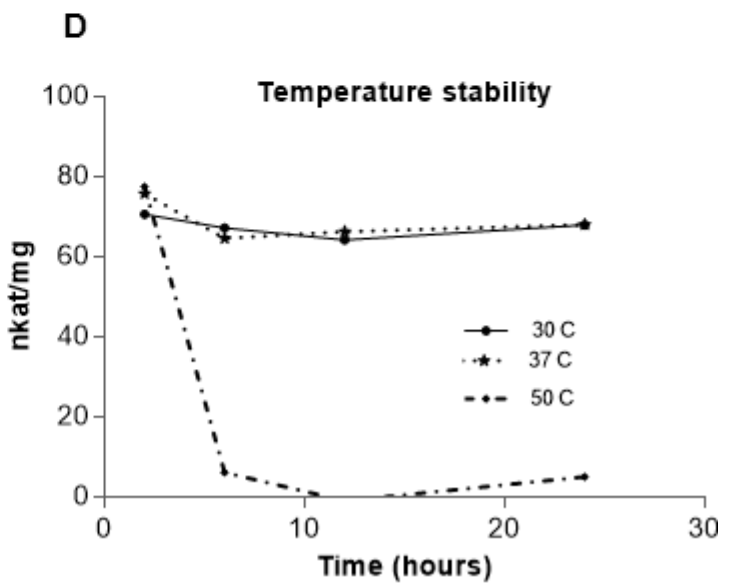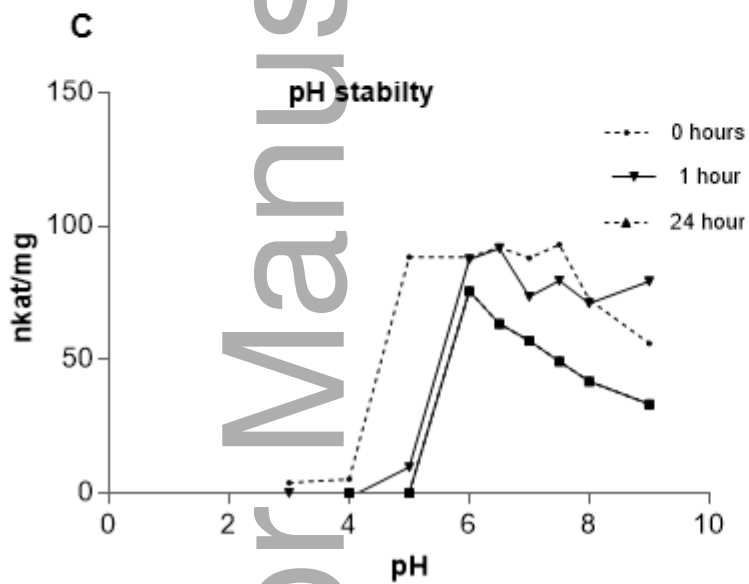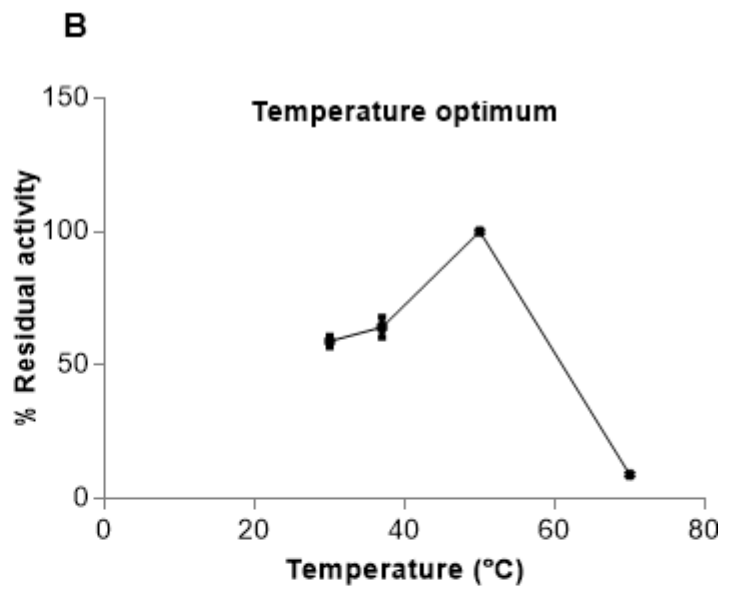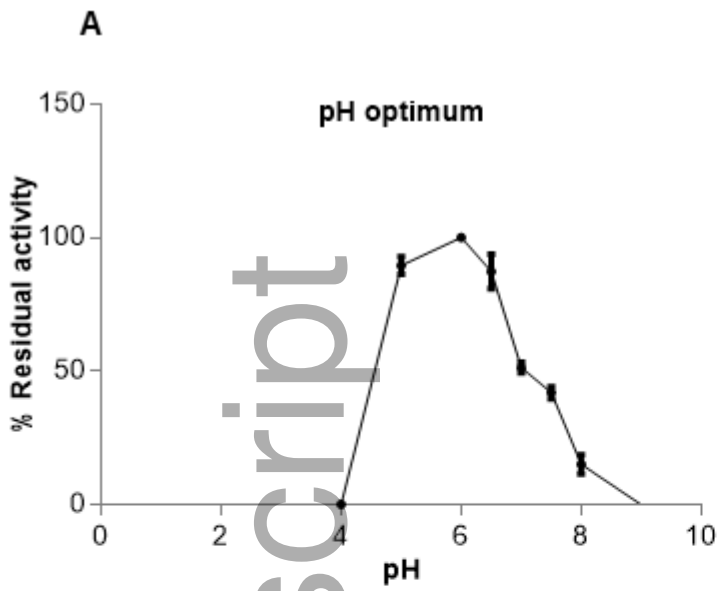
feb2_12250_f3.tif

feb2_12250_f4.tif

feb2_12250_f5.tif

feb2_12250_f6.tif